IEEE Access
Multidisciplinary | Rapid Review | Open Access Journal

Received December 28, 2020, accepted January 13, 2021, date of publication January 19, 2021, date of current version January 28, 2021.

Digital Object Identifier 10.1109/ACCESS.2021.3052933

Optimizing the Solar PV Tilt Angle to Maximize the Power Output: A Case Study for Saudi Arabia

RIDHA BEN MANSOUR[1], MEER ABDUL MATEEN KHAN[1], FAHAD ABDULAZIZ ALSULAIMAN[1,2], AND RACHED BEN MANSOUR[2]

[1]Center of Research Excellence in Renewable Energy, King Fahd University of Petroleum and Minerals, Dhahran 31261, Saudi Arabia
[2]Mechanical Engineering Department, King Fahd University of Petroleum and Minerals, Dhahran 31261, Saudi Arabia

Corresponding author: Ridha Ben Mansour (ridha.benmansour@kfupm.edu.sa)

This work was supported by the King Fahd University of Petroleum and Minerals through the DSR project under Grant SR181027.

ABSTRACT Estimation of solar radiation distribution is crucial for the performance, design, and economic evaluations of solar panels and/or collector systems operating under various climatic conditions, tilt angles, and geographic locations. A comprehensive study involving the combined effect of tilt angle as well as ambient temperature for maximizing the PV array power output was performed. At first, we present a comparison between different isotropic and anisotropic models showing that the anisotropic model gains 5% more energy than the isotropic one. We report monthly and yearly optimum tilts derived from the anisotropic model. Utilizing the optimum tilt derived from the selected anisotropic model, a case study of a mono-crystalline silicon PV array with 2.76 kWp of the rated power is carried out to evaluate the PV performance in five cities of the Kingdom of Saudi Arabia. The results show that the estimated yearly optimum tilt angle is close to the latitude of the studied cities. For the city of Dhahran, a gain of 4.2% power generation is achieved at ambient temperature through monthly adjustment of the PV module instead of yearly adjustment. The estimated yearly tilt angles are as follow: 27.3° for Dhahran, 26.0° for Riyadh, 22.7° for Jeddah, 32.7° for Arar, and 20.1° for Abha. Although Riyadh and Arar receive the same annual average GHI of 6.0 kW/m^2, the yearly average PV power output is ∼7.1% higher for Arar (1.50kW) compared with Riyadh (1.40 kW). This is mainly attributed to the fact that Riyadh has a higher annual average ambient temperature of 29°C compared with 23°C for Arar. Thus, in addition to panel orientation, the ambient temperature was found to have a significant impact on the performance of the PV system and should be taken into consideration when designing the system.

INDEX TERMS Solar radiation, solar PV, modeling, optimum tilt angle, maximum power generation.

NOMENCLATURE

ABBREVIATIONS AND SYMBOLS

AST	Atlantic Standard Time, °degrees
GHI	Global Horizontal Irradiance, W/m^2
G_T	Solar radiation reaching on PV surface, ° W/m^2
G_{sc}	Solar constant, W/m^2
H_B	Beam radiation, W/m^2
H_D	Diffuse radiation, W/m^2
H_B	Beam radiation, W/m^2
H_g	Monthly average daily solar radiation, W/m^2
H_T	Total solar radiation, W/m^2
H_R	Reflected radiation, W/m^2
$\bar{H}_o$	Extraterrestrial radiation, W/m^2
I_D	Diode current, A
I_{photo}	Photo-generated current, A
I_o	Reverse saturation current, A
I_{pv}	PV module current, A
K_T	Clearness Index
LOCE	Levelized cost of electricity, US$ / kWh
n	Day of the year
N_S	Number of cells in series
P_{max}	Maximum power, W
PV	photovoltaic
P_{pv}	PV output power, V
RE	Renewable energy
R_N	Shunt resistance, Ω
Rs	Series resistance, Ω
T_a	Ambient temperature, °C
T_c	Cell temperature, °C

The associate editor coordinating the review of this manuscript and approving it for publication was Shravana Musunuri.

U_L	Coefficient of heat transfer to the environment, kW/m2°C
V	Voltage. °C

GREEK LETTERS

α	Solar absorption of the module
β	PV tilt angle, °degrees
β_{mopt}	Monthly optimal tilt,°degrees
β_{yopt}	Yearly optimal tilt,°degrees
δ	Declination angle,°degrees
θ	Incident angle, °degrees
θ_z	Azimuth angle,°degrees
τ	Solar transmittance of the module
φ	Latitude,°degrees
ω	Solar hour angle, °degrees
ω_{ss}	Sunset hour angle,°degrees

I. INTRODUCTION

Solar photovoltaic (PV) energy has been increasingly popular among renewable energy (RE) sources during the last decade. This is due to the fact that major fossil fuel resources are being continuously depleted and are having a detrimental effect on global climate change. Unlike some traditional power sources, solar PV power generation is a clean source of energy that does not contribute to the carbon footprint on the environment. In 2018, 11% of the total global energy consumption came from modern renewables while 80% of global energy consumption came from fossil fuels [1]. Until 2018, the share of renewables in electricity generation was 26% and it is expected to reach 38% by 2030 [2]. In 2019, a total RE capacity of 2,588 GW has been installed, including 633 GW (24.5%) from solar resources and 651 GW (25.2%) from wind resources. The remaining 1303 GW (50.4%) came from other resources including hydropower, geothermal energy, biopower, and ocean power (Fig. 1) [1]. Solar PV accounts for 24.2 % (627 GW) of global RE capacity, while solar thermal energy accounts for only 0.2 % (6 GW). China, Japan, USA, Germany, and India are the top five leaders in terms of installed solar PV, accounting for 71% of total solar PV installations worldwide [3]. Solar PV capacity is predicted to reach 2,840 GW by 2030 and 8,519 GW by 2050 [4]. The levelized cost of electricity (LCOE) for solar PV has dropped significantly during the last decade, reaching USD 0.068/kWh in2019 compared with USD 0.37/kWh in 2010 [5]. With engineering and technology advancing, LCOE is expected to continue to decrease, falling in the range USD 0.014–0.05/kWh by 2050 [4]. The Gulf Cooperation Council (GCC) region has an immense RE potential, and particularly solar PV. As a result, significant growth in renewables boosted the region's power supply during the last decade. Solar power technology has been advancing and emerging in the region as cost-competitive during 2016-2018, compared with traditional energy technology. In 2019, UAE was leading in the GCC region with 1783 MW of installed solar PV,

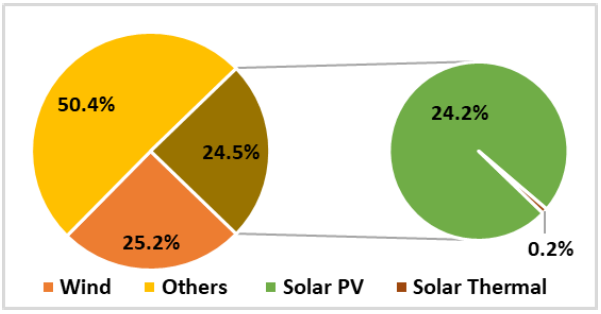

FIGURE 1. Global RE capacity share from different sources.

followed by Saudi Arabia and Kuwait with 344 MW and 43 MW respectively[3].

Saudi Arabia has an abundant solar resource with an average annual solar radiation of ∼2,200 kWh/m^2 [6]. Global Horizontal Irradiance (GHI) varies through the Arabian Peninsula ranging from 3.7-7.9 kWh/m^2/day and 4.1-7.5 kWh/m^2/day for the east and west coast respectively, while the central part receives 4.0-7.7 kWh/m^2/day [7]. As a result, a significant addition of solar PV took place in the kingdom during the last 10 years, reaching 344 MW by 2019. The KSA has set a goal towards deployment of RE in general and solar PV in particular, to reach a planned capacity of 20 GW by 2023 and 40 GW by 2030, as stated by the Renewable Energy Project Development Office [8].

Measuring the amount of solar radiation at a given location is essential for the design and economic assessment of the PV system, yet long-term data is usually not available for many places in the world. Indeed, various empirical models based on available climate data have been developed to estimate solar energy availability and many researchers have attempted to present models and algorithms for estimating solar radiation on a tilted surface for various geographic locations and weather conditions [9]. These models have similar mathematical representations of solar radiation calculation except for the diffuse sky radiation component, which is usually classified into isotropic and anisotropic models. Isotropic diffuse models are based on radiation intensity alone and do not take into account the orientation, while the anisotropic models consider the circumsolar diffuse and/or the horizontal-brightening components on a sloped surface [10], [11]. Reviews on some of the isotropic (Liu and Jordan, Karonakis, Badescu), and anisotropic models (Hay and Davies (HD), Reindle, and Hay & Davies Klucher Reindle (HDKR)) have been reported in [10], [12], [13]. While determining the optimum tilt angle for Canada, Hailu and Fung [14] concluded that the isotropic model gave lower tilt angle estimates relative to the latitude of the location, compared with slightly higher tilt angle estimates for the anisotropic model. Similarly, the anisotropic model achieved a higher tilt angle for various locations in India [15]. Shukla *et al.* [16] performed another study in India using three isotropic and three anisotropic models. The estimated radiation output was higher with respect to the other two isotropic models, while lower compared with the anisotropic

models. HD and HDKR both used the anisotropic model and estimated slightly higher values compared to Liu and Jordan, while also achieving similar results for cloudy weather conditions [17]. In two studies, one by Kaddoura *et al.* [11] performed for Saudi Arabia, and another by Calbaro [18] performed for Italy, the anisotropic models demonstrated effective results for both the summer and winter months, while the isotropic models showed reliable results for the summer months only.

The performance of the PV system is affected by several factors such as module efficiency and module characteristics; climatic conditions (humidity, temperature, solar radiation); geographic location (latitude); ground reflection properties; panel orientation and tilt angle [19], [20]. These parameters are critical for the degree of solar radiation absorbed by the panels and for the PV performance, as the PV power output is a function of the orientation angle and the amount of solar radiation falling on the tilted surface. Subsequently, proper installation and operation of PV systems with high performance can be achieved upon considering the above-mentioned factors.

A variety of mathematical models and correlations have been developed by researchers to predict the optimum tilt angle of the PV for achieving maximum power output [12]. A review of different models and optimization techniques (i.e. genetic algorithm (GA), particle swarm optimization (PSO), artificial neural network (ANN)) for estimating the optimum tilt angle in different geographic locations was presented in the literature [10]. A detailed study on maximizing PV power performance, particularly in a desert environment was performed by Abdeen *et al.* [21]. Monthly, seasonal, and yearly optimum tilt angles for PV modules have been estimated in Oman [22], where the fixed single axis yearly tilt angle was 27° (latitude +3 degrees). A similar study for the city of Madinah yielded a yearly tilt of 23.5°, corresponding to the latitude of the site of 24.5° for a single-axis tracking [23]. Tilt angle optimization studies for four cities in Malaysia delivered about a 4% increase in power output by monthly optimum tilt adjustment [13]. An optimum tilt angle for 18 cities of Saudi Arabia was identified and obtained that the yearly optimum tilt angle is close to the latitude of the city [24]. Siraki and Pillay conducted a study on tilt angle optimization for various latitudes in urban environments, considering the effects of shading [25]. The optimum PV tilt angle was estimated for several countries using photovoltaic software and NREL's PVWatts program [26], [27]. Mekhlief *et al.* studied the effects of dust, humidity, and air velocity on PV cells, and reported that all of these factors have a combined effect on the radiation reaching on a tilted surface and thus should not be studied individually [28].

In the above-mentioned studies ([10], [11], [12] [15], [17], [18] and [26]), researchers have made significant contributions in developing both isotropic and anisotropic estimation models for solar radiation reaching on a tilted surface. Most of the researchers usually focus on obtaining the yearly optimum tilt angle for a single location and then use it as a representative for the whole country [26]. For a country like Saudi Arabia, where meteorological conditions vary significantly in different locations, estimating a single average optimum tilt angle is not representative for the whole country. It is well-documented in literature that PV power output is not only a function of the tilt angle but also of PV cell temperature [36]. Taking into consideration both the solar radiation incident on a titled surface and the temperature effects, can improve the amount of power generation and reduce the cost of solar energy systems as well as the cost of energy produced. That is why a comprehensive study involving the combined effect of tilt angle and ambient temperature for maximizing the PV array power output in various locations in KSA is of major importance. Since no such study has been performed so far and to the best of the author's knowledge, and the need for a comprehensive approach is much required especially for harsh environment regions like KSA. Here, a detailed mathematical model for obtaining monthly and yearly optimum PV panel tilt angles for yielding maximum power output is presented, based on monthly average solar radiation and ambient temperature data. Thereafter, a case study was presented to analyze the effects of solar radiation, optimum tilt angle, and PV module temperature on the PV array power generation in five cities in KSA with different climatic conditions. This study shall help domestic and commercial PV installers to more accurately design their system which should ultimately generate more power from the solar energy conversion system.

This section discusses the importance of the study conducted by reviewing the past literature in the relevant field. Section II highlights the brief mathematical modeling for optimizing the tilt angle and the model for cell temperature subjected to solar radiation. The methodology of the proposed approach is discussed in section III, followed by the results and discussion of the case study performed in section IV. Finally, section V emphasizes the study outcomes and reflects the importance of the study that benefits the local PV designers.

II. SOLAR RADIATION MATHEMATICAL MODEL

Solar energy is directly converted into electrical energy using solar PV panels. The amount of electric energy produced is a function of the amount of solar energy striking the panel surface. Hence, it is imperative to understand the relation between the sun position and the surface tilt angle of the panel [29]. Several methods for optimizing the tilt angle have been proposed, including manual and automatic solar tracking methods that employ various mathematical models reported in [11], [12], [33]–[38], [13], [22]–[24], [29]–[32]. Here, a mathematical model for optimization of the tilt for a sloped surface is briefly described. Further detailed modeling can be found in [31], [36].

A. SOLAR TIME AND ANGLES

As the sun is the primary source of solar energy from the radiation emitted from the sun, the energy received from the

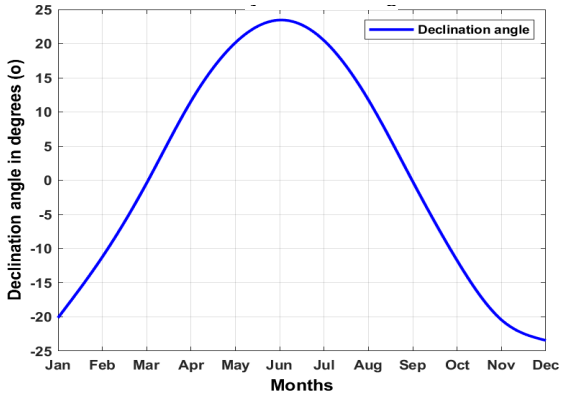

FIGURE 2. Declination angle for any location.

sun per unit of time on a unit area is the solar constant (G_{sc}). A value for solar constant adopted by the World Radiation Center (WRC) is 1367 W/m^2 [36].

1) DECLINATION ANGLE AND ANGLE OF INCIDENCE

The polar axis or the earth rotation axis is tilted or inclined at an angle of 23.45° with respect to the earth's elliptical orbit. The declination angle (δ) is defined as the angle between the perpendicular plane to a line between the sun and the earth, and the earth's elliptical orbit. This angle ranges between -23.45° to +23.45°. The degree variation throughout the year is calculated using the Cooper equation [39], as expressed in "(1)". The variation of the declination angle throughout the year is shown in Fig. 2.

$$\delta = 23.45 sin\left(360\frac{(284+n)}{365}\right) \tag{1}$$

where n is the nth day of the year.

The incident angle (θ) is the angle formed by the sun's beam or rays and the normal to that surface at which the beam strikes. Equation (2) is used for the estimation of the incident angle on a horizontal surface.

$$\cos(\theta) = \sin(\varphi)\sin(\delta) + \cos(\varphi)\cos(\delta)\cos(\omega) \tag{2}$$

where, φ is the latitude of the location and ω is the hour angle. For a tilted surface in the northern hemisphere facing south, "(2)" can be written as "(3)":

$$\cos(\theta) = \sin(\varphi-\beta)\sin(\delta) + \cos(\varphi-\beta)\cos(\delta)\cos(\omega) \tag{3}$$

where, β is the slope angle between the plane and surface at which the radiation is incident.

2) HOUR ANGLE AND SOLAR AZIMUTH ANGLE

The solar hour angle (ω) is based on the nominal time of 24h required for the sun to rotate 360 ° around the earth. Hence the hour angle at solar noon will be zero, with each 15° representing one hour. The hour angle can be represented by "(4)" and obtained from Atlantic Standard Time (AST), where the positive value corresponds to afternoon hours and the negative value corresponds to morning hours.

$$\omega = 15\,(AST - 12) \tag{4}$$

The solar azimuth angle (γ_s) is defined as the angle between the projection of the sun's rays or beam radiation on a horizontal plane. The solar azimuth angle can be estimated by the following relation "(5)".

$$\gamma_s = sign(\omega)\left|\cos^{-1}\left(\frac{\cos(\theta_z)\sin(\varphi) - \sin(\delta)}{sin(\theta_z)\cos(\varphi)}\right)\right| \tag{5}$$

where, θ_z is the zenith angle expressed in "(6)".

$$\cos(\theta_z) = \sin(\varphi)\sin(\delta) + \cos(\varphi)\cos(\delta)\cos(\omega) \tag{6}$$

3) SUNRISE AND SUNSET ANGLES AND DAY LENGTH

The sunrise and sunset angles for the northern hemisphere can be derived from "(6)" when the zenith angle is zero ($\theta_z = 0$), and hence sunset hour angle is given by "(7)."

$$\omega_{ss} = min\begin{cases}\cos^{-1}(-\tan(\varphi)\tan(\delta)) \\ \cos^{-1}(-\tan(\varphi-\beta)\tan(\delta))\end{cases} \tag{7}$$

The day length (hours from sunrise to sunset) can be expressed by "(8)."

$$N = \frac{2}{15}\cos^{-1}(-\tan(\varphi)\tan(\delta)) \tag{8}$$

B. TOTAL SOLAR RADIATION

The total solar radiation (H_T) incident on a sloped surface is the sum of three contributions of solar radiation: beam radiation (H_B), diffuse radiation (H_D) and ground reflected radiation (H_R).

$$H_T = H_D + H_B + H_R \tag{9}$$

Equation (9) can further be arranged as "(10)."

$$H_T = H_d R_d + (H_g - H_d)R_b + H_g\rho_g\left(\frac{1-\cos(\beta)}{2}\right) \tag{10}$$

where, H_d is given by the relation with monthly fraction of diffuse ($\bar{H}_d/\bar{H}$). The radiation incident on the global horizontal surface is defined by H_g. The terms R_b and R_d are the ratios of the average daily beam and diffuse radiation on a tilted surface, respectively. R_b is defined by the ratio of the cosine of the angle of incidence to the cosine of zenith angle.

$$R_b = \frac{cos(\theta)}{\cos(\theta_z)} \tag{11}$$

The ratio (R_b) can be expanded using "(3)" and "(6)", for surfaces in the northern hemisphere tilted towards the equator, represented by "(12)".

$$R_b = \frac{\sin(\varphi-\beta)\sin(\delta) + \cos(\varphi-\beta)\cos(\delta)\cos(\omega)}{\sin(\varphi)\sin(\delta) + \cos(\varphi)\cos(\delta)\cos(\omega)} \tag{12}$$

R_d, can be expressed by using different isotropic and anisotropic models. Liu and Jordan's isotropic model [40] can be expressed as in "(13)."

$$R_d = \left(\frac{1+\cos(\beta)}{2}\right) \tag{13}$$

Badescu isotropic diffuse model can be written as "(14)"[16]

$$R_d = \left(\frac{3 + \cos(2\beta)}{4}\right) \tag{14}$$

Hay and Davies (HD) [17], [36] proposed an anisotropy index defined by a function of transmittance of the atmosphere for beam radiation. Anisotropy index is represented as H_B/H_o. This model estimates fraction of diffuse component which is usually circumsolar and assumes it to be in the same direction as beam radiation. HD is given by the relation "(15)," where "H_O" monthly average daily extraterrestrial radiation.

$$R_d = \frac{H_B}{H_O} R_b + \left(1 - \frac{H_B}{H_O}\right)\left(\frac{1 + \cos(\beta)}{2}\right) \tag{15}$$

Reindel *et al.* have modified the Hay and Davies model by the addition of a horizontal- brightening term, which can be defined as $f = \sqrt{(H_B/H_g)}$, proposed by Klucher [17], [36]. The modified Hay and Davies referred to as HDKR anisotropic model is represented by, "(16)."

$$R_d = \frac{H_B}{H_O} R_b + \left(1 - \frac{H_B}{H_O}\right)\left(\frac{1 + \cos(\beta)}{2}\right) \times \left(1 + \sqrt{\frac{H_B}{H_g}} \sin^3\left(\frac{\beta}{2}\right)\right) \tag{16}$$

1) EXTRATERRESTRIAL RADIATION

At any time between sunrise and sunset, the incident solar radiation (G_o) on a horizontal surface outside of the atmosphere of the earth is defined as the normal incident solar radiation divided by the average daily beam (R_b) and it is given by the following approximate relationship expressed in "(17)."

$$G_o = G_{SC}\left(1 + 0.033\cos\frac{360\,n}{365}\right)(\sin(\varphi)\sin(\delta) + \cos(\varphi)\cos(\delta)\cos(\omega)) \tag{17}$$

The monthly average daily extraterrestrial radiation ($\bar{H}_o$) on a horizontal surface is obtained by integrating "(17)" over day length. Therefore, $\bar{H}_o$ can be estimated as "(18)."

$$\bar{H}_o = \frac{24 * 3600 * G_{SC}}{\pi}\left(1 + 0.033\cos\frac{360\,n}{365}\right) \times \left(\frac{\pi\,\omega_{ss}}{180}\sin(\varphi)\sin(\delta) + \cos(\varphi)\cos(\delta)\sin(\omega_s)\right) \tag{18}$$

Since the units of G_{SC} is defined by Watt per square meter, the $\bar{H}_o$ is in joules per square meter per day.

2) CLEARNESS INDEX

The monthly average clearness index is defined by Liu and Jordan [40], as the ratio of the monthly average daily radiation on a horizontal ($\bar{H}$) to that of monthly average daily extraterrestrial radiation ($\bar{H}_o$).

$$\bar{K}_T = \frac{\bar{H}}{\bar{H}_o} \tag{19}$$

where the monthly average fraction of the diffuse component is calculated based on the correlations described in "(20)" [36].

$$\frac{\bar{H}_d}{\bar{H}} = \begin{cases} (a)1.391 - 3.560\bar{K}_T + 4.189\bar{K}_T^2 - 2.137\bar{K}_T^3, \\ for\,\omega_{ss} \le 81.4^\circ \text{ and } 0.3 \le \bar{K}_T \le 0.8 \\ (b)1.311 - 3.022\bar{K}_T + 3.427\bar{K}_T^2 - 1.821\bar{K}_T^3, \\ f \text{ or } \omega_{ss} > 81.4^\circ \text{ and } 0.3 \le \bar{K}_T \le 0.8 \end{cases} \tag{20}$$

C. PV POWER GENERATION

The power generation from solar PV array, which is the product of the voltage and current, depends on the solar radiation impinging on a tilted surface, the ambient temperature, and the PV module characteristics.

1) PV CELL TEMPERATURE MODEL

The solar module efficiency is substantially affected by the ambient temperature, as the module temperature can increase when it is exposed to high solar radiation, resulting in temperature-induced power loss, as well as PV cell delamination and rapid degradation. The maximum increase in temperature will be at midday while the module temperature in the evening will be the same as the ambient temperature. In this work, the PV cell temperature is estimated as a function of the ambient temperature, heat loss to the environment, electrical conversion efficiency, and irradiance variation. It is obtained by applying the energy balance equation on a unit area of the module which is cooled by losses to the environment.

$$\tau\alpha G_T = \eta_c G_T + U_L\,(T_c - T_a) \tag{21}$$

Because, the solar transmittance of the PV module (τ), the solar absorption of the module (α), and the coefficient of heat transfer to the environment (U_L) are difficult to measure and to control, additional information beyond that supplied by the manufacturer is proposed for nominal operating cell temperature (NOCT). By substituting the standard values at NOCT conditions (incident radiation of 0.8 kW/m^2), in "(19)," and assuming that the efficiency varies linearly with cell temperature and can be written as "(22)", shown at the bottom of the next page [41]. where, $G_{T,NOCT}$ is the solar radiation at which NOCT is defined (800W/m^2)

$T_{a,NOCT}$ is the ambient temperature at which NOCT is defined (20°C)

$T_{c,NOCT}$ is the nominal operating module temperature ranging from 45°C to 48°C

$T_{c,STC}$ is the temperature of the module under STC condition (25°C)

$\eta_{mp,STC}$ is the efficiency for maximum power point (13.5 %)

α_p is the temperature coefficient of power (−0.46%/°C)

τ is solar transmittance of any cover over PV module ($\tau = 90\%$)

α is solar absorption of PV module ($\alpha = 90\%$)

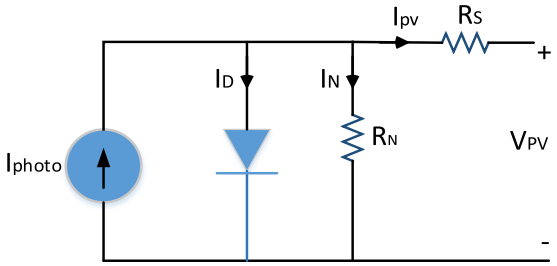

FIGURE 3. PV cell single diode model.

2) PV MODULE POWER OUTPUT MODEL

A PV cell can be modeled as a single diode model where a current source is in parallel with the diode as shown in Fig. 3 [42]. The P-V and I-V characteristics of a PV cell exhibit a nonlinear relationship because of the cell temperature and radiation intensity. The detailed model for PV can be found in [31], [36], and [43]. A single diode approach was adopted in this study.to determine the I-V curves due to its simplicity and good accuracy [44].

At a fixed temperature and solar radiation, the fundamental equation describing the I-V characteristics of a cell single diode of this model is given by "(23)."

$$I_{pv} = I_{photo} - I_o \left[exp\left(\frac{\left(V_{pv} + I_{pv}R_s\right) e}{kT_cNs} \right) - 1 \right] - \frac{V_{PV} + I_{PV}R_S}{R_N} \quad (23)$$

And the power output defined as the product of current and the voltage is given by "(24)."

$$P_{pv} = I_{pv} * V_{pv} \quad (24)$$

where,

e is electronic charge (e = 1.602×10^{-19}C)

k is Boltzmann's constant (k = 1.381×10^{-23}J/K)

This circuit of the single-diode model requires five variables to be evaluated. Additional parameters available in cell datasheets provided by the PV manufacturers have been used to determine the PV output. These parameters generally include the nominal open-circuit voltage, the nominal short-circuit current, the voltage at the Maximum power point (MPP), the open-circuit voltage/temperature coefficient, the short circuit current/temperature coefficient, and they are given with reference to standard reference conditions, as shown in Table 5.

The reverse saturation current (I_o) depends on the temperature and it is assumed to vary linearly with the cell temperature and consequently resistance and current parameters

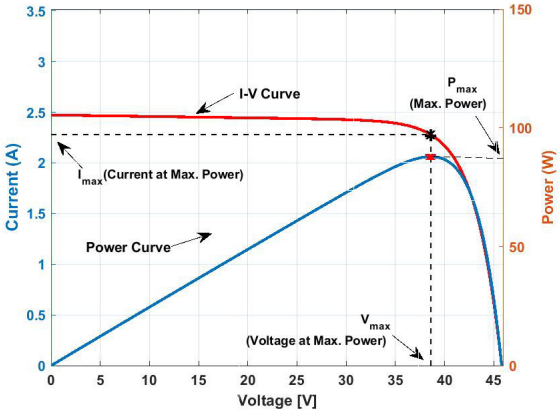

FIGURE 4. Typical I-V and P-V performance curves for a PV module.

(Rs, R_N, I_o, I_{photo}) can be estimated by considering the three remarkable points of the I-V curve [43]. The general I-V equation at the maximum power can be found in "(25)." A typical current-voltage and power- voltage performance curve is shown in Fig. 4.

$$P_{max} = \left(I_{pv} - I_o \left[exp\left(\frac{(V_{max} + I_{max}R_s)\, e}{kT_cNs} \right) - 1 \right] - \frac{V_{max} + I_{max}R_S}{R_N} \right) V_{max} \quad (25)$$

III. METHODOLOGY

For estimating the maximum power generated by a tilted solar PV array for any given location, we used MATLAB simulations. A flow chart (Fig. 5) highlights the key steps in determining the maximum power from a PV array. The first step involves obtaining the latitude (φ); ambient air temperature (T_a); monthly average daily solar radiation (H_g) of the location of choice; and the day of the year (n). Upon selection of the location, the declination angle (δ), incident angle (θ), and sunset hour angle (ω_{ss}) were estimated using "(1)" to "(7)", followed by calculation of the clearness index (K_T) and extraterrestrial radiation (H_o) for all 365 days of the year. All the above parameters shall be calculated for a range of slopes values (β) ranging from 0 to 90^0. A decision block decides whether the sunset hour angle ($\omega_{ss} \leq 81.4$) is satisfied or not, and based on this condition the monthly diffuse fraction is calculated using two equations described in "(20)". To obtain the optimum tilt angle, the total solar radiation (H_T) hitting the surface is calculated for varying tilt angles (β) through the year. The optimum tilt angle for each day is estimated upon searching for slope values at which the maximum total solar radiation is achieved. The computed

$$T_c = \frac{T_a + (T_{c,NOCT} - T_{a,NOCT}) \left(\frac{G_T}{G_{T,NOCT}}\right) \left[1 - \frac{\eta_{mp,STC}(1-\alpha_p T_{c,STC})}{\tau\alpha}\right]}{1 + (T_{c,NOCT} - T_{a,NOCT}) \left(\frac{G_T}{G_{T,NOCT}}\right) \left[\frac{\alpha_p \eta_{mp,STC}}{\tau\alpha}\right]} \quad (22)$$

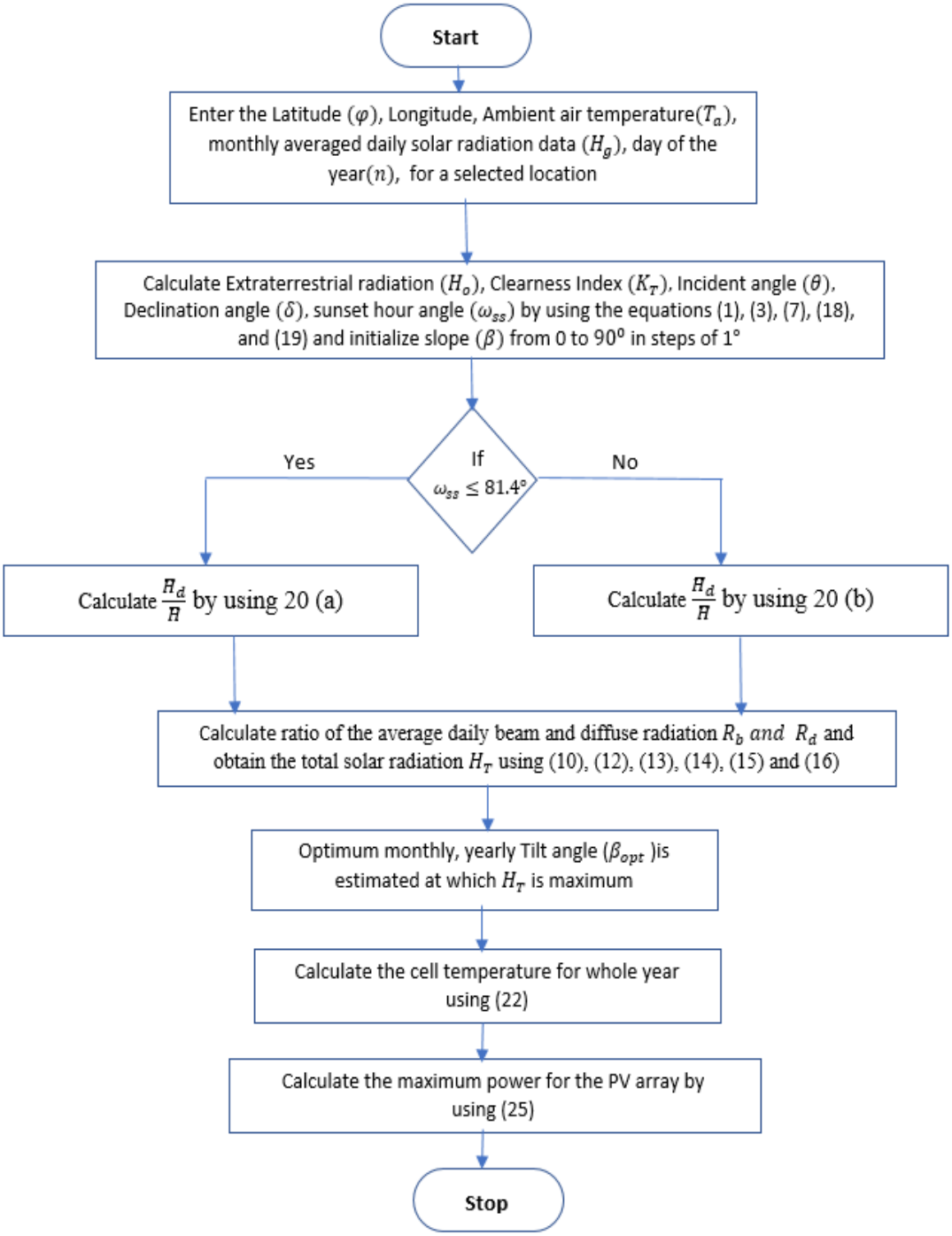

FIGURE 5. Flowchart showings the steps involved in optimizing the tilt angle to generate maximum power from PV array.

tilt angle with maximum average total radiation serves as the average monthly optimum tilt (β_{mopt}) and yearly optimum tilt (β_{yopt}) for PV. The total solar radiation and the optimum tilt angle are estimated as monthly averages for twelve months. The cell temperature is then calculated using the average monthly optimum tilt and the solar radiation of the selected location using "(22)". The PV array consists of parallel series of connected panels as shown in Fig. 6. The arrays are arranged in six parallel sets of two PV panels connected in series so that they have a rated peak power of 2.76 kWp. The power temperature coefficient of -0.46 %/K and the efficiency for maximum power point 13.5 % for each panel are used in simulations. Further details for the specifications of the PV cell and array are provided in appendix A. The PV array power output is estimated for both monthly optimum tilt and yearly optimum tilt by varying voltage until the maximum

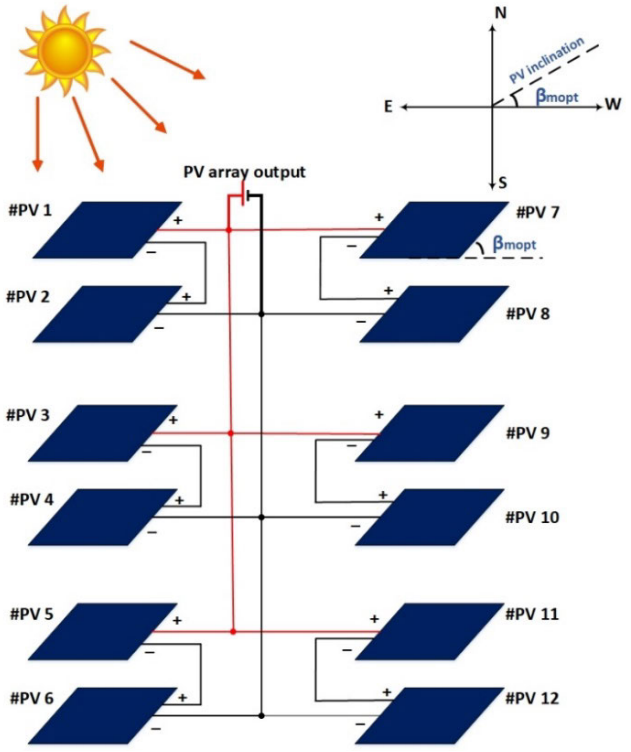

FIGURE 6. The PV array system and tilt angle.

power is found. The effects of solar radiation and module cell temperature are studied throughout the year under different levels of radiation.

IV. RESULTS AND DISCUSSION

The mathematical model for maximizing solar radiation input, estimating the optimum tilt angle, and consequently generating maximum PV array power, was developed in MATLAB. The latitude and longitude, ambient air temperature, and global horizontal irradiance recorded as monthly average daily solar radiation was collected from renewable resource ATLAS, King Abdullah City for Atomic and Renewable Energy (K·A·CARE) [7]. Based on the data collected from the source, total solar radiation reaching on a tilted surface, diffuse radiation, beam radiation, reflected radiation, and optimum tilt angle for all 365 days was estimated. The first case study was for the city of Dhahran where the monthly average daily global, diffused, and beam solar radiation were estimated considering two isotropic and two anisotropic models. The model that proved to be the most accurate was used as the basis for a second case study, which attempts a comprehensive comparison between five cities in KSA.

A. DHAHRAN CITY

In this section, a case study is presented for estimating the maximum PV array power generation for Dhahran, a city located in the eastern region of Saudi Arabia. The weather station was located on the campus of King Fahd University

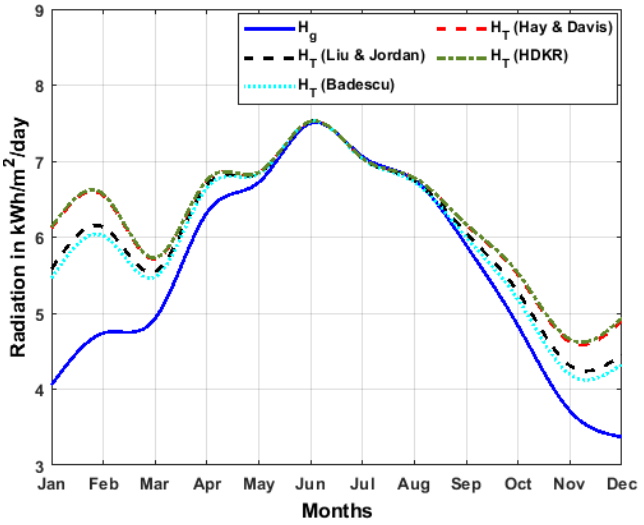

FIGURE 7. Monthly average global horizontal radiation (H_g) and total solar radiation (H_T) for two isotropic and two anisotropic models for Dhahran.

of Petroleum and Minerals at 26.30355°N and 50.14412°E. The monthly average daily solar radiation (H_g) for Dhahran (Fig. 7) is in the range 3.4-7.5 kWh/m^2 for the twelve months of the year, with the highest radiation recorded in June. The maximum temperature was recorded in July at 37.4 °C, and the minimum was recorded in January at 16.6 °C. The average annual ambient temperature was 28.1 °C. Table 1 presents the monthly average daily global horizontal radiation, ambient temperature, and the monthly and yearly optimum tilt angle obtained for Dhahran using 4 empirical models (two isotropic and two anisotropic). In general, the total solar radiation on a tilted surface obtained with these models is an improvement over the total solar radiation reaching on a horizontal surface, as depicted in Fig. 7 and Table 1.

The comparison of monthly average daily solar radiation on a tilted surface revealed that all selected four models demonstrated similar results during the summer season. Anisotropic models (HD and HDKR) on the other hand yielded better results during the winter compared with the isotropic models (Liu and Jordan and Badescu models) (Fig. 7). In January for instance, the Liu and Jordan model estimated monthly average radiation of 5.6 kWh/m^2, while the HDKR model estimated 6.1 kWh/m^2, ∼9% gain compared with the isotropic model. Similarly, the lowest annual average horizontal solar radiation was estimated using the isotropic diffuse models by Badescu (5.95 kWh/m^2 -day), followed by Liu and Jordan (6.01 kWh/m^2-day), while the anisotropic models (HD and HDKR) demonstrated higher annual values of 6.2 kWh/m^2-day, which amounts to 3.5% and 5% energy gain respectively. This can be explained by the addition of the circumsolar and horizontal-brightening components in the isotropic diffuse model. The contribution of these components has a more pronounced effect on global solar radiation in winter months when the skies are cloudy. Under clear weather conditions (in summer), the diffused fraction of solar

TABLE 1. Monthly calculated cell temperature, monthly and yearly optimum tilt for Dhahran city.

Months	Monthly Average daily radiation (kWh/m^2)	Ambient Temperature ($^{\circ}C$)	Liu and Jordan (isotropic)		Badescu (isotropic)		Hay & Davies (anisotropic)		HDKR (anisotropic)	
			Total Radiation H_T (kWh/m^2)	Monthly average optimum Tilt (β_{mopt})	Total Radiation H_T (kWh/m^2)	Monthly average optimum Tilt (β_{mopt})	Total Radiation H_T (kWh/m^2)	Monthly average optimum l Tilt (β_{mopt})	Total Radiation H_T (kWh/m^2)	Monthly average optimum Tilt (β_{mopt})
Jan	4.1	16.6	5.6	46.0	5.5	43.8	6.1	49.3	6.1	49.7
Feb	4.7	19.3	6.1	37.7	6.0	34.5	6.5	41.0	6.6	41.6
Mar	4.9	22.0	5.5	25.6	5.5	21.5	5.7	28.5	5.7	29.4
Apr	6.3	27.7	6.7	15.4	6.7	13.0	6.7	17.0	6.8	17.3
May	6.7	33.6	6.8	6.6	6.8	5.4	6.9	7.3	6.9	7.4
Jun	7.5	36.0	7.5	2.5	7.5	2.2	7.5	2.9	7.5	2.9
Jul	7.1	37.4	7.0	4.5	7.0	3.7	7.0	4.9	7.0	4.9
Aug	6.8	37.0	6.7	12.1	6.7	10.1	6.8	13.1	6.8	13.3
Sep	5.9	34.6	6.1	22.5	6.0	19.1	6.2	24.5	6.2	25.2
Oct	4.8	31.3	5.3	33.4	5.2	29.2	5.5	36.3	5.5	37.5
Nov	3.7	23.9	4.3	42.1	4.2	38.1	4.6	45.6	4.7	47.1
Dec	3.4	17.7	4.4	46.8	4.3	43.9	4.9	50.6	4.9	51.7
Average	5.5	28.1	6.0	24.6	5.9	22.0	6.2	26.7	6.2	27.3

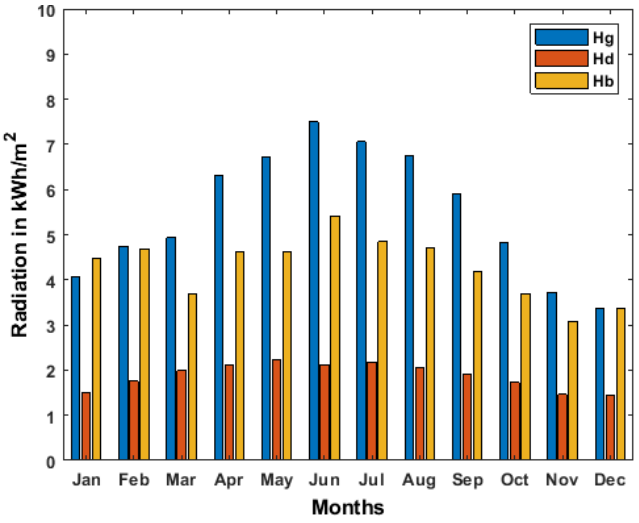

FIGURE 8. Monthly solar radiation, diffuse radiation, and beam radiation calculated for Dhahran city.

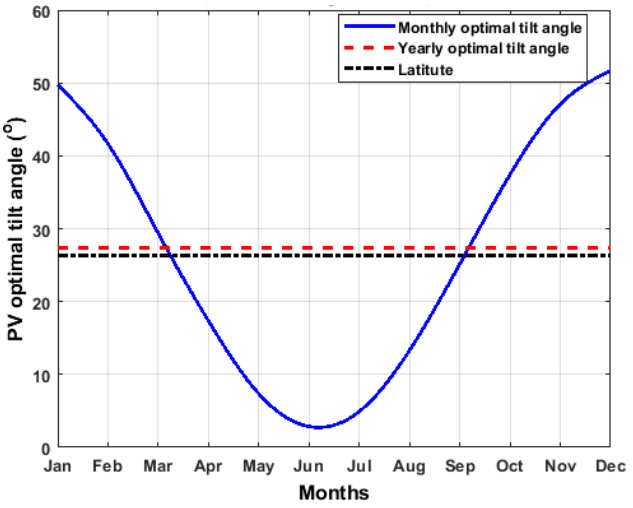

FIGURE 9. Monthly and yearly optimum tilt angle obtained for Dhahran city.

radiation is assumed to be scattered and anisotropic models gave the same results as the isotropic model. The obtained results agree with References [11] and [18]. The monthly optimum tilt angles derived from all models show that the peak of solar radiation is in June and the minimum in December. The monthly optimum tilt angle ranges from 2° (corresponds to June) to 52° degrees (December) as depicted in Table 1. Anisotropic models predicted a slightly higher optimum tilt angle compared with isotropic models. For instance, the yearly optimum tilt achieved by HDKR, Hay and Davies, Liu and Jordan, and Badescu models, was 27.33°, 26.74°, 24.6°, and 22.04°, respectively. Furthermore, the yearly optimum tilt estimated by isotropic models was slightly lower than the latitude of Dhahran, while the anisotropic model estimated a slightly higher tilt angle. The results we obtained are in fair agreement with the results in [14].

Upon comparative analysis of four models, the HDKR model was selected in the further study while isotropic models are simple and give the most conservative estimates as demonstrated in this study, many theoretical and experimental studies have shown that HDKR produces results that are closer to the experimentally observed values [11], [18], [23], and [34]. The results of estimated solar radiation, optimum tilt angle for Dhahran city using the HDKR anisotropic model are shown in Figs. 8-10. The bar graph (Fig. 8) shows the monthly average daily solar radiation for global horizontal radiation, diffuse radiation, and beam radiation. The beam component represents the major contribution in obtaining total solar radiation on a tilted surface. Fig. 9 shows that for maximum energy available to be achieved, the monthly optimum tilt angle during the summer season should be lower than the latitude of the location, while higher during the winter. Further, the yearly tilt value obtained for the city of Dhahran was 27.33°, which is 1.04 times the latitude of the location. As shown in Fig. 10, the monthly adjustment of the PV module generates more solar radiation output compared

TABLE 2. Maximum power, voltage, and current obtained for a single PV panel inclined at monthly and yearly optimum tilted using HDKR model.

Months	Monthly Average daily radiation (kWh/m^2)	PV Cell Temperature ($^{\circ}C$)	Monthly optimum Tilt (β_{mopt})				Yearly optimum Tilt ($\beta_{yopt} = 27.3$)				% gain in power output between monthly and yearly tilt
			V_{max} (V)	I_{max} (A)	P_{max} (W)	PV array output in kW	V_{max} (V)	I_{max} (A)	P_{max} (W)	PV array output in kW	
Jan	4.1	34.0	38.7	3.2	125.6	1.51	38.8	3.0	116.3	1.40	8.0%
Feb	4.7	36.4	38.4	3.3	126.9	1.52	38.5	3.2	123.0	1.48	3.1%
Mar	4.9	37.1	37.9	2.7	102.0	1.22	37.9	2.7	101.8	1.22	0.2%
Apr	6.3	42.6	37.3	3.0	111.3	1.34	37.3	2.9	109.8	1.32	1.4%
May	6.7	48.7	36.4	2.9	104.7	1.26	36.4	2.7	99.6	1.20	5.1%
Jun	7.5	53.1	35.9	3.1	110.9	1.33	35.9	2.9	102.8	1.23	7.9%
Jul	7.1	53.5	35.7	2.9	104.3	1.25	35.7	2.7	98.0	1.18	6.5%
Aug	6.8	53.0	35.8	2.9	105.3	1.26	35.8	2.9	102.6	1.23	2.6%
Sep	5.9	49.3	36.3	2.8	103.0	1.24	36.3	2.8	102.7	1.23	0.2%
Oct	4.8	43.9	37.0	2.7	100.3	1.20	37.0	2.7	98.8	1.19	1.5%
Nov	3.7	36.6	37.8	2.4	91.3	1.10	37.8	2.3	86.5	1.04	5.5%
Dec	3.4	33.2	38.4	2.6	101.5	1.22	38.4	2.4	93.1	1.12	9.1%
Average	5.5	43.5				1.29				1.24	4.2%

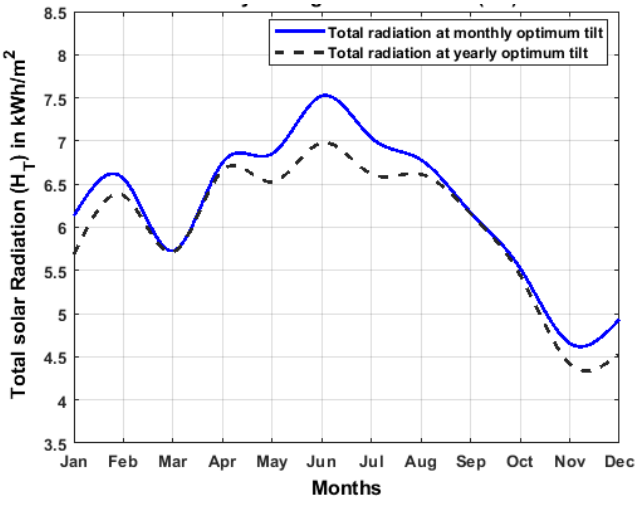

FIGURE 10. Total solar radiation striking the slope surface of PV defined by monthly and yearly optimum tilt.

with yearly adjustment. Variations in PV cell temperature is a function defined by ambient temperature and the monthly optimum tilt are shown in Fig. 11 and Table 2. The maximum cell temperature obtained was 53.5 °C for the month of July (ambient temperature 37.4 °C), and the minimum cell temperature obtained was 33.2 °C for December (ambient temperature 17.7 °C). The average annual cell temperature was estimated to be 43.5 °C, showing an approximately 55% increase in temperature when compared to the annual average ambient temperature.

The V-I and P-V characteristics of the PV panel tilted at an angle defined by monthly and yearly tilt, operating under real weather conditions were evaluated based on the HDKR model. The characteristics show the varying nature of the current and power when subjected to monthly variations in solar radiation and temperature. Additionally, the locus of maximum power is presented for each month. The effects of temperature and solar radiation on the PV module characteristics are shown in Fig. 12. In general, increasing cell temperature for a given radiation range leads to slightly decreased voltage and output power (Fig. 12). In July, the estimated module power of a PV module adjusted at monthly tilt was 104.3 W upon receiving solar radiation of 7.1 kWh/m^2, while having a maximum cell temperature of 53.5 °C. However in February, the PV power was estimated to be 126.9 W after receiving minimal solar radiation of 4.7 kWh/m^2 and having cell temperature of 36.4 °C. This clearly shows the strong negative correlation between PV cell temperature and the amount of power output. By selecting a monthly optimum tilt angle, maximum module power output was achieved in February (126.9 W), while minimal in November (91.3 W).

The PV power generated for the whole PV array system consisting of twelve PV panels was also studied. The average power output from the PV array tilted at both monthly and yearly optimum angle is presented in Table 2 and Fig. 13. During the year, maximum power was achieved in January and February with about 1.52 kW. The maximum yield in power output at monthly optimal tilt was in December, accounting for 9.1% more energy compared with the yearly optimal tilt. Although the radiation level was lowest in December (3.4 kWh/m^2 day), the PV module temperature was also minimal (33.2°C) for that month, and as a result, the month of December yielded more PV power than any other month. The yearly average power estimated from the PV array was 1.29 kW and 1.24 kW for monthly and yearly optimum tilt adjustment respectively, as presented in Table 2. It was reported that the monthly optimum tilt estimated 4.2% more power output than the yearly optimum tilt of PV.

B. MULTI-LOCATIONS

The objective of this section is to analyze the effects of latitude and climatic conditions (temperature and solar radiation) on the optimum tilt angle of PV panels in KSA, and the related maximum energy generation from a PV array system. Five locations were chosen, covering regions with various climatic conditions in the eastern, central, western, northern,

TABLE 3. Monthly data of solar radiation, ambient temperature, and PV module temperature of different cities.

Month	Dhahran (26.3° N, 50.14° E)			Riyadh (24.7° N, 46.67° E)			Jeddah (21.5° N, 39.24° E)			Arar (31.0° N, 40.9° E)			Abha (18.2° N, 42.54° E)		
	GHI (kW/m^2/day)	Air Temp. (°C)	PV cell Temp. (°C)	GHI (kW/m^2/day)	Air Temp. (°C)	PV cell Temp. (°C)	GHI (kW/m^2/day)	Air Temp. (°C)	PV cell Temp. (°C)	GHI (kW/m^2/day)	Air Temp. (°C)	PV cell Temp. (°C)	GHI (kW/m^2/day)	Air Temp. (°C)	PV cell Temp. (°C)
Jan	4.1	16.6	34.0	4.7	16.8	36.6	4.6	24.9	42.9	3.6	9.9	28.1	4.4	13.0	28.3
Feb	4.7	19.3	36.4	5.4	21.0	40.3	5.4	26.3	44.4	4.6	12.4	31.6	6.3	14.8	35.1
Mar	4.9	22.0	37.1	5.8	23.8	41.1	5.8	28.3	44.9	6.0	16.7	36.2	7.1	18.5	38.3
Apr	6.3	27.7	42.6	6.6	28.9	45.8	6.6	28.9	45.4	7.3	21.2	40.4	5.6	16.5	30.3
May	6.7	33.6	48.7	7.0	35.2	51.6	7.0	33.3	49.7	7.8	28.7	46.8	6.7	21.6	37.2
Jun	7.5	36.0	53.1	8.0	37.5	55.6	7.3	33.3	50.0	8.4	31.4	49.9	6.9	24.2	40.2
Jul	7.1	37.4	53.5	7.9	38.9	56.9	7.3	35.5	52.4	8.4	35.2	53.7	5.8	22.9	36.3
Aug	6.8	37.0	53.0	7.2	39.4	56.6	6.5	36.0	51.4	7.4	35.8	53.4	6.1	21.8	36.3
Sep	5.9	34.6	49.3	6.4	35.9	52.7	6.1	34.6	50.3	6.3	33.0	49.9	6.1	21.8	37.2
Oct	4.8	31.3	43.9	5.3	32.0	48.0	5.4	33.1	48.8	4.9	26.5	42.3	6.7	18.4	37.3
Nov	3.7	23.9	36.6	4.1	22.2	36.3	4.6	29.6	45.2	3.7	15.9	31.4	5.5	15.3	33.2
Dec	3.4	17.7	33.2	3.8	15.8	31.5	3.8	25.6	39.7	3.3	9.0	25.6	5.5	15.0	35.1
Avg	5.5	28.1	43.5	6.0	29.0	46.1	5.9	30.8	47.1	6.0	23.0	40.8	6.1	18.7	35.4

TABLE 4. Comparison of monthly and yearly optimum tilt angle of five cities of KSA.

Month	Dhahran (26.3° N 50.1° E)			Riyadh (24.7° N, 46.67° E)			Jeddah (21.5° N, 39.24° E)			Arar (31.0° N, 40.9° E)			Abha (18.2° N, 42.54° E)		
	Monthly tilt	Yearly tilt	PV array output (kW)	Monthly tilt	Yearly tilt	PV array output (kW)	Monthly tilt	Yearly tilt	PV array output (kW)	Monthly tilt	Yearly tilt	PV array output (kW)	Monthly tilt	Yearly tilt	PV array output (kW)
Jan	49.7		1.51	48.4		1.71	44.7		1.50	54.7		1.62	40.7		1.35
Feb	41.6		1.52	40.3		1.64	36.8		1.50	46.9		1.69	33.7		1.77
Mar	29.4		1.22	28.5		1.45	24.8		1.36	35.5		1.69	22.1		1.70
Apr	17.3		1.34	15.8		1.39	12.4		1.35	22.9		1.63	8.5		1.20
May	7.4		1.26	5.9		1.31	2.6		1.32	12.6		1.48	0.6		1.32
Jun	2.9	27.3	1.33	1.3	26.0	1.42	0	22.7	1.34	7.7	32.7	1.50	0	20.1	1.34
Jul	4.9		1.25	3.5		1.41	0.8		1.34	10.1		1.47	0		1.13
Aug	13.3		1.26	11.9		1.34	8.2		1.22	18.7		1.40	4.8		1.22
Sep	25.2		1.24	23.9		1.34	20.1		1.26	30.7		1.36	16.7		1.30
Oct	37.5		1.20	36.2		1.29	32.7		1.26	42.9		1.31	30.2		1.63
Nov	47.1		1.10	45.7		1.19	42.5		1.27	52.6		1.35	39.6		1.55
Dec	51.7		1.22	50.3		1.36	46.6		1.18	56.8		1.48	44.0		1.75
Avg	27.3		1.29	26.0		1.40	22.7		1.33	32.7		1.50	20.1		1.44

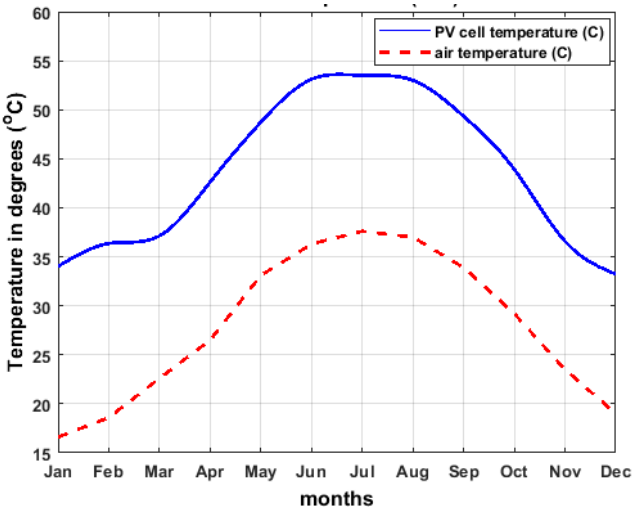

FIGURE 11. PV module temperature subjected to ambient air temperature.

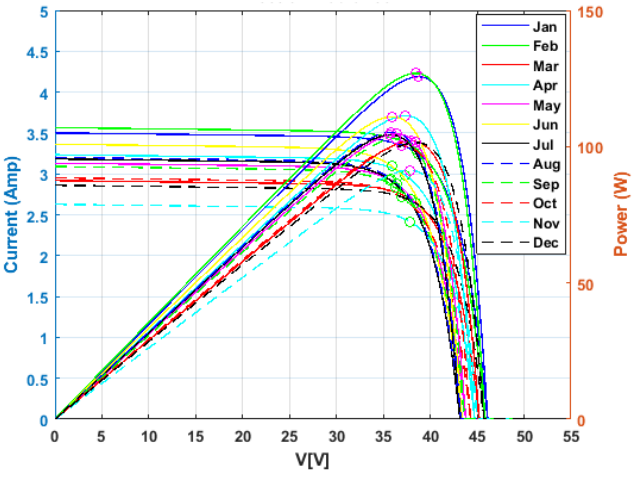

FIGURE 12. I-V and P-V characteristics for a PV module for a tilted surface at the yearly optimal tilt.

and southern regions of KSA. Saudi Arabia spans over a relatively large territory and includes regions with varying weather conditions in terms of humidity and ambient temperature. The city of Dhahran, for example, is representative for hot and humid environments, Abha exhibits relatively low temperatures, while the climate in Riyadh is hot and dry. The geographic locations of the studied cities in KSA are as follows:

1) Dhahran – Eastern region (26.3° N, 50.14° E)
2) Riyadh – Central region (24.7° N, 46.67° E)
3) Jeddah – Western region (21.5° N, 39.24° E)
4) Arar – Northern Region (31.0° N, 40.9° E)
5) Abha – Southern Region (18.2 °N, 42.54° E)

Table 3 provides monthly variations of daily solar radiation, ambient temperature, and PV module temperatures of the studied cities. Fig. 14 shows the average monthly

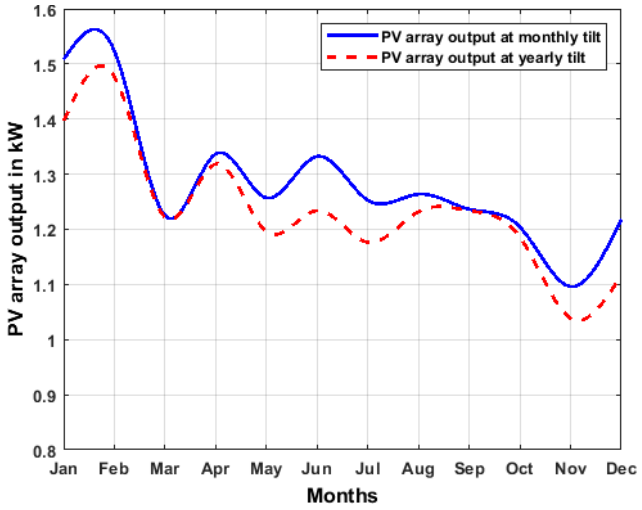

FIGURE 13. Monthly PV output power inclined at monthly optimum tilt and yearly optimum tilt.

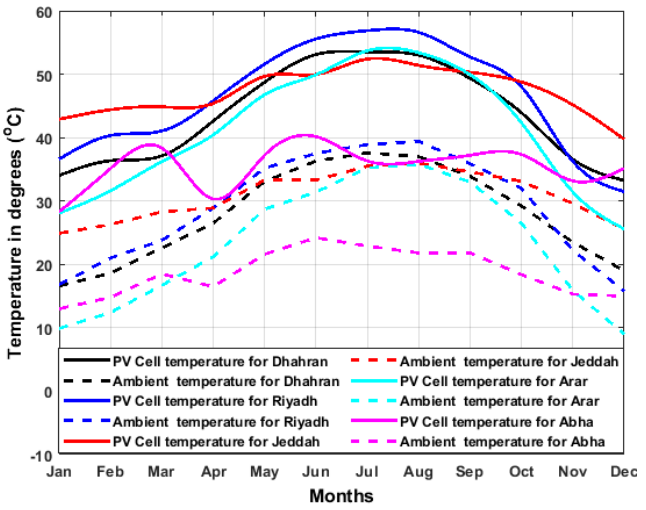

FIGURE 15. PV module temperature profile subjected to an ambient air temperature of five cities.

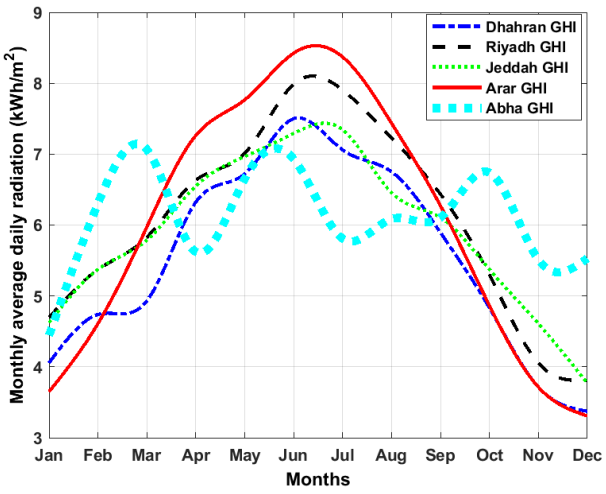

FIGURE 14. Monthly average daily radiation for five selected cities.

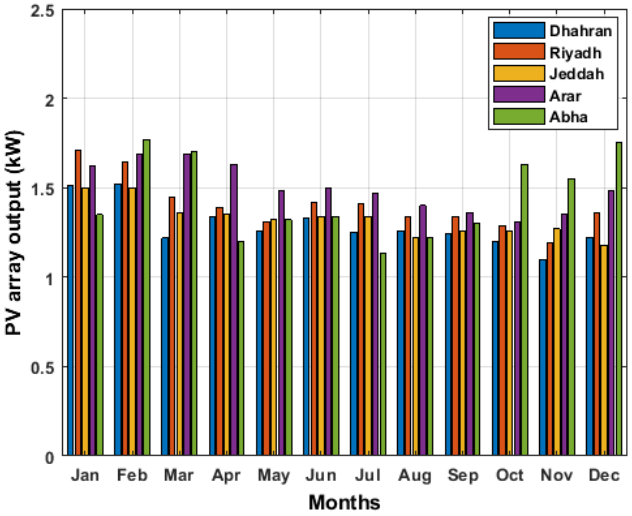

FIGURE 16. Monthly average PV array output of five selected locations of KSA.

daily solar radiation on a horizontal surface. As shown in Table 3, of all the studied locations the city of Arar receives the highest GHI values during the months June-July (up to 8.4 kWh/m^2/day), and the lowest GHI during the winter season (3.3 kWh/m^2/day). For the cities of Riyadh, Jeddah, and Arar, the monthly average maximum ambient temperature was recorded in August and was 39.4 °C, 36 °C, 35.8 °C respectively. Similarly for Dhahran, the maximum ambient temperature was recorded to be 37.4 °C in July and Abha recorded 24.2°C in June. The PV module temperature profiles subjected to ambient temperature for the five studied cities are shown in Fig. 15. Riyadh city recorded the maximum PV module temperature of 56.9 °C in the peak summer month of July, resulting in decreased maximum power efficiency. Compared with the rest of the studied locations, for the month of July, the city of Abha recorded the lowest PV module temperature of 36.3°C.

Fig. 16 shows the monthly average PV array power output for the studied locations and Table 4 shows the PV array power output achieved using monthly optimum tilt. The yearly tilt for Dhahran, Riyadh, Jeddah, Arar, and Abha was estimated to be 27.3°, 26.0°, 22.7°, 32.7°, and 20.1° respectively. The maximum PV array power generated in Dhahran (1.52 kW), Jeddah (1.50 kW), Arar (1.69 kW) and Abha (1.77 kW) was in February, while in Riyadh the maximum was achieved in January (1.71 kW). Although Riyadh and Arar receive the same annual average GHI of 6.0 kW/m^2, the yearly average PV power output is ∼7.1% higher for Arar (1.50 kW) compared with Riyadh (1.40 kW). This is mainly attributed to the fact that Riyadh has a higher annual average cell temperature of 46.1°C compared with 40.8°C for Arar. Jeddah on the other hand, a city with a very similar GHI of 5.9 kWh/m^2, was estimated at 1.33 kW average annual power output-lower, compared with estimations for

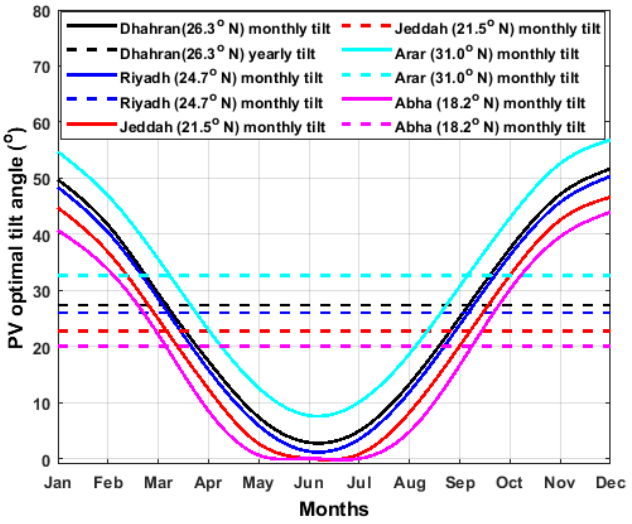

FIGURE 17. Monthly and yearly tilt angle for five cities.

both Arar and Riyadh. Again, the reduction in power output is mainly attributed to the high cell temperatures in Jeddah and confirms the negative correlation between temperature and PV power output. The monthly and yearly tilt angles of the studied locations in KSA are depicted in Fig. 17. Table 4 clearly shows that the optimum yearly tilt angle is consistently very similar to the latitude of the location.

V. CONCLUSION

This study is focused on obtaining data pertaining to the monthly and yearly optimum PV panel tilt angle for yielding maximum power generation from a PV array system, considering the effect of ambient temperature for different locations in Saudi Arabia. The total solar radiation on a tilted surface was estimated by using both isotropic and anisotropic models. While both models demonstrated similar values for the summer season, the anisotropic model yielded slightly higher values for the winter season. The developed approach based on the HDKR model was used effectively for understanding the combined effects of solar radiation, tilt angle, and ambient temperature on the PV power output estimation in five cities in KSA. The yearly tilt for Dhahran (26.3°N, 50.14°E), Riyadh (24.7°N, 46.67°E), Jeddah (21.5°N, 39.24°E), Arar (31.0° N, 40.9°E), and Abha (18.2°N, 42.54° E) was estimated to be 27.3°, 26.0°, 22.7°, 32.7°, and 20.1° respectively. The results reveal that the estimated yearly optimum tilt angle is approximately equal to the latitude of the studied cities in KSA. Further, it was demonstrated that the monthly adjustment of the PV module generates more solar output compared with yearly adjustment. A gain of 4.2% power generation can be achieved for Dhahran at the ambient temperature by monthly adjustment of the PV module instead of yearly adjustment. Compared with the rest of the studied locations, Dhahran received the lowest yearly average solar radiation (5.5 kW/m^2/day) and generated the least energy (1.29 kW), 16.2% lower than the maximum PV output obtained for Arar city. The effects of air temperature on power output can be revealed in locations with similar yearly average solar incident radiation values like Riyadh and Arar. The latter exhibits a gain of 7.1% power generation compared to Riyadh.

Although this study is representative for a small size PV system rated power of 2.76 kWp, the results are valuable and applicable for large PV systems also. The study lays a road map for commercial and residential PV installers to further optimize their PV system and effectively contribute to reducing the LCoE for PV installations. Finally, it is highly recommended that along with the tilt angle and ambient temperature effects on PV power output, the impact of dust and shading should also be taken into consideration in order PV system to be more productive.

APPENDIXES

APPENDIX A

TABLE 5. PV array specifications.

Parameter	Symbol	Value
Number of PV cells	N_s	72
Open Circuit voltage	V_{oc}	48.7 V
Short circuit current	I_{SC}	5.99 A
Rated voltage at maximum power	V_{mpp}	41.0 V
Rated current at maximum power	I_{max}	5.61 A
Maximum power	P_{max}	230 W
Power temperature coefficient	μ_P	-0.46 % / K
Voltage temperature coefficient	μ_{ocv}	132.5 mV / K
Current temperature coefficient	μ_{sc}	3.5 mA / K
Series-connected panel	N_{ser}	2
Parallel-connected Panel	N_{par}	6

ACKNOWLEDGMENT

The authors would like to thank K·A ·CARE for providing the station data for conducting the study.

REFERENCES

[1] *Renewables 2020 Global Status Report*, REN21, Paris, France, 2020.
[2] *Global Renewables Outlook: Energy Transformation 2050*, Int. Renew. Energy Agency, Abu Dhabi, United Arab Emirates, 2020.
[3] *Renewable Capacity Statistics 2020*, Int. Renew. Energy Agency, Abu Dhabi, United Arab Emirates, 2020.
[4] *Future of Solar Photovoltaic: Deployment, Investment, Technology, Grid Integration and Socio-Economic Aspects (A Global Energy Transformation: Paper)*, Int. Renew. Energy Agency, Abu Dhabi, United Arab Emirates, 2019.
[5] *Renewable Power Generation Costs in 2019*, Int. Renew. Energy Agency, Abu Dhabi, United Arab Emirates, 2020.
[6] A. Hepbasli and Z. Alsuhaibani, "A key review on present status and future directions of solar energy studies and applications in Saudi Arabia," *Renew. Sustain. Energy Rev.*, vol. 15, no. 9, pp. 5021–5050, Dec. 2011.
[7] K. A. Care, King Abdullah City for Atomic and Renewable Energy, Saudi Arabia. *Renewable Resource Atlas*. Accessed: 2015. [Online]. Available: https://rratlas.energy.gov.sa/
[8] KSA Ministry of Energy. *Overview of Saudi Arabia's Renewable Energy Program*. Accessed: 2019. [Online]. Available: https://www.powersaudiarabia.com.sa/web/index.html
[9] S. A. Klein and J. C. Theilacker, "An algorithm for calculating monthly-average radiation on inclined surfaces," *J. Sol. Energy Eng.*, vol. 103, no. 1, pp. 29–33, Feb. 1981.
[10] A. K. Yadav and S. S. Chandel, "Tilt angle optimization to maximize incident solar radiation: A review," *Renew. Sustain. Energy Rev.*, vol. 23, pp. 503–513, Jul. 2013.

[11] T. O. Kaddoura, M. A. M. Ramli, and Y. A. Al-Turki, "On the estimation of the optimum tilt angle of PV panel in saudi arabia," *Renew. Sustain. Energy Rev.*, vol. 65, pp. 626–634, Nov. 2016.
[12] A. Z. Hafez, A. Soliman, K. A. El-Metwally, and I. M. Ismail, "Tilt and azimuth angles in solar energy applications—A review," *Renew. Sustain. Energy Rev.*, vol. 77, pp. 147–168, Sep. 2017.
[13] T. Khatib, A. Mohamed, M. Mahmoud, and K. Sopian, "Optimization of the tilt angle of solar panels for Malaysia," *Energy Sources, A, Recovery, Utilization, Environ. Effects*, vol. 37, no. 6, pp. 606–613, Mar. 2015.
[14] G. Hailu and A. S. Fung, "Optimum tilt angle and orientation of photovoltaic thermal system for application in greater Toronto area, Canada," *Sustainability*, vol. 11, no. 22, p. 6443, Nov. 2019.
[15] P. Yadav and S. S. Chandel, "Comparative analysis of diffused solar radiation models for optimum tilt angle determination for Indian locations," *Appl. Sol. Energy*, vol. 50, no. 1, pp. 53–59, Jan. 2014.
[16] K. N. Shukla, S. Rangnekar, and K. Sudhakar, "Comparative study of isotropic and anisotropic sky models to estimate solar radiation incident on tilted surface: A case study for Bhopal, India," *Energy Rep.*, vol. 1, pp. 96–103, Nov. 2015.
[17] A. Q. Jakhrani, A. Othman, A. R. H. Rigit, S. R. Samo, and S. Ahmed, "Estimation of incident solar radiation on tilted surface by different empirical models," *Int. J. Sci. Res. Publ.*, vol. 2, no. 12, pp. 15–20, 2012.
[18] E. Calabrò, "The disagreement between anisotropic-isotropic diffuse solar radiation models as a function of solar declination: Computing the optimum tilt angle of solar panels in the area of Southern-Italy," *Smart Grid Renew. Energy*, vol. 03, no. 04, pp. 253–259, 2012.
[19] A. Glick, N. Ali, J. Bossuyt, M. Calaf, and R. B. Cal, "Utility-scale solar PV performance enhancements through system-level modifications," *Sci. Rep.*, vol. 10, no. 1, pp. 1–9, Dec. 2020.
[20] A. Al-Bashir, M. Al-Dweri, A. Al-Ghandoor, B. Hammad, and W. Al-Kouz, "Analysis of effects of solar irradiance, cell temperature and wind speed on photovoltaic systems performance," *Int. J. Energy Econ. Policy*, vol. 10, no. 1, pp. 353–359, Jan. 2020.
[21] E. Abdeen, M. Orabi, and E.-S. Hasaneen, "Optimum tilt angle for photovoltaic system in desert environment," *Sol. Energy*, vol. 155, pp. 267–280, Oct. 2017.
[22] H. A. Kazem, T. Khatib, and A. A. K. Alwaeli, "Optimization of photovoltaic modules tilt angle for oman," in *Proc. IEEE 7th Int. Power Eng. Optim. Conf. (PEOCO)*, Jun. 2013, pp. 703–707.
[23] M. Benghanem, "Optimization of tilt angle for solar panel: Case study for Madinah, Saudi Arabia," *Appl. Energy*, vol. 88, no. 4, pp. 1427–1433, Apr. 2011.
[24] H. Z. Al Garni, A. Awasthi, and D. Wright, "Optimal orientation angles for maximizing energy yield for solar PV in Saudi Arabia," *Renew. Energy*, vol. 133, pp. 538–550, Apr. 2019.
[25] A. Gharakhani Siraki and P. Pillay, "Study of optimum tilt angles for solar panels in different latitudes for urban applications," *Sol. Energy*, vol. 86, no. 6, pp. 1920–1928, Jun. 2012.
[26] M. Z. Jacobson and V. Jadhav, "World estimates of PV optimal tilt angles and ratios of sunlight incident upon tilted and tracked PV panels relative to horizontal panels," *Sol. Energy*, vol. 169, pp. 55–66, Jul. 2018.
[27] R. Abdallah, A. Juaidi, S. Abdel-Fattah, and F. Manzano-Agugliaro, "Estimating the optimum tilt angles for south-facing surfaces in palestine," *Energies*, vol. 13, no. 3, p. 623, Feb. 2020.
[28] S. Mekhilef, R. Saidur, and M. Kamalisarvestani, "Effect of dust, humidity and air velocity on efficiency of photovoltaic cells," *Renew. Sustain. Energy Rev.*, vol. 16, no. 5, pp. 2920–2925, Jun. 2012.
[29] T. M. Yunus Khan, M. E. M. Soudagar, M. Kanchan, A. Afzal, N. R. Banapurmath, N. Akram, S. D. Mane, and K. Shahapurkar, "Optimum location and influence of tilt angle on performance of solar PV panels," *J. Thermal Anal. Calorimetry*, vol. 141, no. 1, pp. 511–532, Jul. 2020.
[30] E. D. Mehleri, P. L. Zervas, H. Sarimveis, J. A. Palyvos, and N. C. Markatos, "Determination of the optimal tilt angle and orientation for solar photovoltaic arrays," *Renew. Energy*, vol. 35, no. 11, pp. 2468–2475, Nov. 2010.
[31] I. H. Rowlands, B. P. Kemery, and I. Beausoleil-Morrison, "Optimal solar-PV tilt angle and azimuth: An Ontario (Canada) case-study," *Energy Policy*, vol. 39, no. 3, pp. 1397–1409, 2011.
[32] T. P. Chang, "Output energy of a photovoltaic module mounted on a single-axis tracking system," *Appl. Energy*, vol. 86, no. 10, pp. 2071–2078, Oct. 2009.
[33] A. K. Yadav and H. Malik, "Optimization of tilt angle for installation of solar photovoltaic system for six sites in india," in *Proc. Int. Conf. Energy Econ. Environ. (ICEEE)*, vol. 3, no. 3, Mar. 2015, pp. 8–11.
[34] I. H. Rowlands, B. P. Kemery, and I. Beausoleil-Morrison, "Optimal solar-PV tilt angle and azimuth: An ontario (Canada) case-study," *Energy Policy*, vol. 39, no. 3, pp. 1397–1409, Mar. 2011.
[35] N. Maru and J. Vajpai, "Model based optimization of tilt angle for solar PV panels in Jodhpur," *Int. J. Comput. Appl.*, vol. 975, p. 8887, Dec. 2014.
[36] E. D. Mehleri, P. L. Zervas, H. Sarimveis, J. A. Palyvos, and N. C. Markatos, "Determination of the optimal tilt angle and orientation for solar photovoltaic arrays," *Renew. Energy*, vol. 35, no. 11, pp. 2468–2475, 2010.
[37] M. Kacira, M. Simsek, Y. Babur, and S. Demirkol, "Determining optimum tilt angles and orientations of photovoltaic panels in Sanliurfa, Turkey," *Renew. Energy*, vol. 29, no. 8, pp. 1265–1275, Jul. 2004.
[38] N. Femia, G. Petrone, G. Spagnuolo, and M. Vitelli, "Optimization of perturb and observe maximum power point tracking method," *IEEE Trans. Power Electron.*, vol. 20, no. 4, pp. 963–973, Jul. 2005.
[39] B. W. Scott, "The absorption of radiation in bone," *Australas. Radiol.*, vol. 4, no. 2, pp. 129–132, Dec. 1960.
[40] A. Jordan, "Daily insolation on surfaces tilted towards the equator," *ASHRAE Trans.*, no. 67, pp. 526–541, Oct. 1962.
[41] HOMER. *How HOMER Calculates the PV Cell Temperature*. [Online]. Available: https://www.homerenergy.com/products/pro/docs/latest/how_homer_calculates_the_pv_cell_temperature.html
[42] V. J. Fesharaki, M. Dehghani, J. J. Fesharaki, and H. Tavasoli, "The effect of temperature on photovoltaic cell efficiency," in *Proc. 1st Int. Conf. Emerg. Trends Energy Conserv.*, Nov. 2011, pp. 20–21.
[43] W. Xiao, F. F. Edwin, G. Spagnuolo, and J. Jatskevich, "Efficient approaches for modeling and simulating photovoltaic power systems," *IEEE J. Photovolt.*, vol. 3, no. 1, pp. 500–508, Jan. 2013.
[44] A. F. Murtaza, U. Munir, M. Chiaberge, P. Di Leo, and F. Spertino, "Variable parameters for a single exponential model of photovoltaic modules in crystalline-silicon," *Energies*, vol. 11, no. 8, pp. 1–14, 2018.

RIDHA BEN MANSOUR received the B.S. degree in mechanical engineering from the National Engineering School of Sfax, Tunisia, in 1998, and the M.S. and Ph.D. degrees in mechanical engineering from Moncton University and Sherbrooke University, Canada, in 2004 and 2008, respectively. After that, he worked for three years as a full time Assistant Professor in mechanical engineering at the University of Moncton, Canada. He served as a Research Scientist at CANMET (R&D, Government of Canada) for more than three years before joining the Doosan Water Research and Development Center, Saudi Arabia. He is currently a Research Engineer with the Center of Research Excellence in Renewable Energy, King Fahd University of Petroleum and Minerals (KFUPM). He has conducted and participated in various demonstration projects related to desalination technologies (RO, MSF and MED) and renewable energy applications. His area of expertise includes desalination in GCC, scaling and fouling assessment, design, optimization and piloting, solar driven desalination and techno-economic assessment.

MEER ABDUL MATEEN KHAN received the B.Sc. degree in instrumentation engineering from Osmania University, in 2012, and the M.Sc. degree in electrical engineering from the King Fahd University of Petroleum and Minerals (KFUPM), KSA, in 2016. He was a Research Assistant with KFUPM, Dhahran, KSA, from 2013 to 2015. Later, he joined as Engineer II at the Center of Research Excellence in Renewable Energy, KFUPM, Dhahran, KSA. His research interests include hybrid renewable energy systems (photovoltaic and wind energy system) and its storage applications, modeling and control of microgrid integrated to PV, maximum power tracking of wind turbine and battery storage systems, and renewable energy-based desalination. He is a certified energy auditor (CEA) and has conducted many energy audits of industries and buildings. He was also a member of Association of Energy Engineers (AEE).

FAHAD ABDULAZIZ ALSULAIMAN received the B.Sc. and M.Sc. degrees in mechanical engineering from the King Fahd University of Petroleum and Minerals (KFUPM), in 2001 and 2003, respectively, and the Ph.D. degree in mechanical engineering with a specialty in energy from the University of Waterloo, in 2010. After that, he was with the Center for Clean Water and Clean Energy, MIT, as a Postdoctoral Associate, for one year. He is the Director of the Center of Research Excellence in Renewable Energy and the Center of Excellence in Energy Efficiency, KFUPM. He served as a Visiting Professor with MIT, NUS, and the University of Oxford, in the summer of 2011, 2015, and 2017, respectively. He is a Certified Energy Manager and a Certified Energy Auditor of the AEE. He published more than 100 scientific articles. He holds several patents. His research interests include renewable energy, co-generation, grid-connection of renewable energy, techno-economic studies for energy systems, energy efficiency, and energy policy and regulations.

RACHED BEN MANSOUR received the B.S., M.S., and Ph.D. degrees in mechanical engineering from Purdue University, W. Lafayette, IN, USA, in 1985, 1987, and 1993, respectively. He is currently an Associate Professor with the Mechanical Engineering Department, KFUPM. He has been involved in the MIT-KFUPM collaboration, from 2009 to 2017, during which he has developed with his MIT colleagues, novel systems for leak detection in pipe networks. Over the last ten years, he has worked on carbon capture methods including Oxy-fuel combustion and Adsorption of CO2 using MOFs. He now involved in developing new membranes for hydrogen production from fuel reforming. He has published over 200 journal and conference papers and has been awarded 31 U.S. patents.